Observations of Mkn 421 during 1997 and 1998 in the energy range above 500 GeV with the HEGRA stereoscopic Cherenkov telescope system

F.A. Aharonian[1], A.G. Akhperjanian[7], M. Andronache[4], J.A. Barrio[2,3], K. Bernlöhr[1,*], H. Bojahr[6], I. Calle[3], J.L. Contreras[3], J. Cortina[3], A. Daum[1], T. Deckers[5], S. Denninghoff[2], V. Fonseca[3], J.C. Gonzalez[3], N. Götting[4], G. Heinzelmann[4], M. Hemberger[1], G. Hermann[1,**], M. Heß[1], A. Heusler[1], W. Hofmann[1], H. Hohl[6], D. Horns[4], A. Ibarra[3], R. Kankanyan[1,7], J. Kettler[1], C. Köhler[1], A. Konopelko[1,***], H. Kornmeyer[2], M. Kestel[2], D. Kranich[2], H. Krawczynski[1], H. Lampeitl[1], A. Lindner[4], E. Lorenz[2], N. Magnussen[6], O. Mang[5], H. Meyer[6], R. Mirzoyan[2], A. Moralejo[3], L. Padilla[3], M. Panter[1], D. Petry[2,†], R. Plaga[2], A. Plyasheshnikov[1,***], J. Prahl[4], G. Pühlhofer[1], G. Rauterberg[5], C. Renault[1,‡], W. Rhode[6], A. Röhring[4], V. Sahakian[7], M. Samorski[5], M. Schilling[5], F. Schröder[6], W. Stamm[5], H.J. Völk[1], B. Wiebel-Sooth[6], C. Wiedner[1], M. Willmer[5], and W. Wittek[2]

[1] Max-Planck-Institut für Kernphysik, Postfach 103980, 69029 Heidelberg, Germany
[2] Max-Planck-Institut für Physik, Föhringer Ring 6, 80805 München, Germany
[3] Universidad Complutense, Facultad de Ciencias Físicas, Ciudad Universitaria, 28040 Madrid, Spain
[4] Universität Hamburg, II. Institut für Experimentalphysik, Luruper Chaussee 149, 22761 Hamburg, Germany
[5] Universität Kiel, Institut für Experimentelle und Angewandte Physik, Leibnizstrasse 15–19, 24118 Kiel, Germany
[6] Universität Wuppertal, Fachbereich Physik, Gaußstrasse 20, 42097 Wuppertal, Germany
[7] Yerevan Physics Institute, Alikhanian Br. 2, 375036 Yerevan, Armenia

Abstract. Since its commissioning in fall 1996, the stereoscopic system of Imaging Atmospheric Cherenkov Telescopes (IACTs) of HEGRA, with an energy flux sensitivity νF_{ν} at 1 TeV of $10^{-11}\,\mathrm{erg\,cm^{-2}\,s^{-1}}$ for one hour of observation time, has been used to monitor the BL Lac object Mkn 421 on a regular basis. In this paper, we report detailed temporal and spectral information about the TeV characteristics of Mkn 421 in 1997 and 1998. We study the light curve, the shortest time scales of flux variability, the differential spectra on a diurnal basis for several days with good γ-ray statistics, and the time-averaged energy spectrum. Special emphasis is put on presenting the data taken during the world-wide April 1997 multiwavelength campaign.

Key words: galaxies: BL Lacertae objects: individual: Mkn 421 – gamma rays: observations

Send offprint requests to: Henric Krawczynski

[*] Now at Forschungszentrum Karlsruhe, P.O. Box 3640, 76021 Karlsruhe, Germany

[**] Now at Enrico Fermi Institute, The University of Chicago, 933 East 56th Street, Chicago, IL 60637, USA

[***] On leave from Altai State University, Dimitrov Street 66, 656099 Barnaul, Russia

[†] Now at Universidad Autónoma de Barcelona, Instituto de Física d'Altes Energies, 08193 Bellaterra, Spain

[‡] Now at LPNHE, Universités Paris VI-VII, 4 place Jussieu, 75252 Paris Cedex 05, France

Correspondence to: Henric Krawczynski, Tel.: (Germany) +6221 516 471, (Henric.Krawczynski@mpi-hd.mpg.de)

1. Introduction

The advent of the *Compton Gamma Ray Observatory* and the EGRET instrument has led to the spectacular discovery of intense high energy γ-ray radiation from as many as $\sim$65 Active Galactic Nuclei (AGN) in the 0.1 to 10 GeV energy range (Hartman et al. 1999). The recorded sources belong almost entirely to the blazar population of AGNs, i.e. BL Lac objects, Optically Violent Variables (OVVs), and highly polarized quasars, all radio-loud sources which show variability on short time scales in most of the observed frequency bands. The power emitted in γ-radiation frequently dominates the power radiated by the source (see e.g. the spectral energy distributions shown by Fossati et al. 1998). It is widely believed that the non-thermal γ-ray emission is produced in a relativistic jet by a population of electrons. Synchrotron radiation is emitted at longer wavelengths, and Inverse Compton (IC) radiation from interactions of the highest energy electrons with lower energy seed photons at shorter wavelengths (see for recent reviews Coppi 1997; Sikora 1997; Ulrich et al. 1997). The origin of the IC seed photons has not yet been established. There are several debated possibilities for the dominant target photon population: lower energy synchrotron photons in the Synchrotron Self Compton mechanism (see e.g. Bloom & Marscher 1993; Ghisellini et al. 1996; Mastichiadis & Kirk 1997), or external photons, e.g. radiation from the nuclear continuum scattered or reprocessed in the broad-line regions (Sikora et al. 1994; Blandford & Levinson 1995), or accretion disk photons (Dermer & Schlickeiser 1994). Although these possibilities have been studied in great detail,

models where hadrons are the particles primarily accelerated (see e.g. Mannheim 1993) cannot be ruled out yet. Clearly, the study of the emission process could yield crucial clues regarding the structure of the jets leading ultimately to an understanding of the mechanisms of energy extraction operating in the surroundings of the central supermassive object.

In this paper, we report on the 1997 and 1998 observations of the BL Lac object Mkn 421 (redshift $z = 0.031$) with the IACT system of HEGRA (Daum et al. 1997). The system provides an energy threshold of 500 GeV, an angular resolution of $0.1°$ and an energy resolution of 20% for individual photons, as well as an energy flux sensitivity νF_ν at 1 TeV of 10^{-11} erg cm^{-2}s^{-1} (S/N $= 5\sigma$) for one hour of observation time. TeV observations yield information about the emitting particles with very high energies, complementary to the information from longer wavelengths. Due to the extreme conditions needed for the production of TeV photons, TeV blazars could be extremely revealing laboratories for the understanding of these sources in general. It should be pointed out that the TeV radiation is expected to be partially absorbed by the Diffuse Extragalactic Background Radiation (DEBRA) (e.g. Gould & Schréder 1966; Stecker et al. 1992). While on the one hand the DEBRA extinction opens unique possibilities to infer information about the DEBRA density in the largely unconstrained 0.5 to 50 μm wavelength region (see Aharonian et al. 1999b, called *Paper 2* in the following), on the other hand it renders the understanding of the source more difficult (e.g. Coppi & Aharonian 1999; Bednarek & Protheroe 1999).

The BL Lac Mkn 421 was the first extragalactic object to be discovered as a TeV emitter (Punch et al. 1992; Petry et al. 1996). The early HEGRA observations during the 1994/1995 observation period showed that the spectrum of Mkn 421 was significantly softer than the Crab spectrum (Petry et al. 1996). While the mean TeV flux level of Mkn 421 is about 0.5 Crab units (Petry et al. 1996), flares exceeding five Crab units on timescales as short as 15 minutes have been observed (Gaidos et al. 1996).

The second BL Lac object to be discovered as a TeV source (Quinn et al. 1996; Bradbury et al. 1997), Mkn 501 (redshift $z = 0.034$), underwent a major outburst in the X-ray and in the TeV energy range during 1997 (see e.g. Protheroe et al. 1998). Detailed accounts of the results obtained with the HEGRA IACTs are given in (Aharonian et al. 1999a, called *Paper 1* in the following), Paper 2, and in (Aharonian et al. 1999c). The source emission showed strong variability with differential fluxes at 1 TeV ranging from a fraction to 10 times the Crab flux. The HEGRA IACT system was used to determine diurnal differential spectra for more than 60 individual days. Surprisingly, no correlation between absolute flux and spectral shape was found. The differential time-averaged photon spectrum was well described by a power law with an exponential cutoff $dN/dE \propto (E/1\text{TeV})^{-1.9} \exp(-E/6.2\text{TeV})$ up to energies of ~ 20 TeV. Due to the similarity in redshifts of Mkn 421 and Mkn 501 ($z = 0.031$ and 0.034, respectively) the intergalactic extinction of the TeV photons caused by the DEBRA should be very

similar for both objects and a comparison of both spectra is of utmost interest.

The paper is organized as follows. In Sect. 2 the IACT system of HEGRA is introduced, and in Sect. 3 the data sample and the analysis techniques are described. The results concerning the time-averaged and the diurnal properties, as well as the search for variability within individual nights are presented in Sect. 4. In Sect. 5 the results are summarized and discussed.

2. The HEGRA Cherenkov telescope system

The HEGRA collaboration operates six imaging atmospheric Cherenkov telescopes located on the Roque de los Muchachos on the Canary island of La Palma, at 2200 m above sea level. A prototype telescope (CT1) started operation in 1992 and has undergone significant hardware upgrades since then (Mirzoyan et al. 1994; Rauterberg et al. 1995). This telescope continues to operate as an independent instrument and the Mkn 421 data taken with this telescope will be presented elsewhere. The stereoscopic system of Cherenkov telescopes consists of five telescopes (CT2 - CT6), and has been taking data since 1996, initially with three and four telescopes, and since fall 1998 as a complete five-telescope system. Four of the telescopes (CT2, CT4, CT5, CT6) are arranged in the corners of a square with roughly 100 m side length, and one telescope (CT3) is located in the center of the square. During 1997 and 1998, when the data discussed in this paper were taken, CT2 was still used as a stand alone detector.

The telescopes have an 8.5 m^2 tessellated reflector, focusing the Cherenkov light onto a camera with 271 Photomultipliers (PMTs) which cover a field of view of $4.3°$ in diameter. A telescope is triggered when the signal in at least two adjacent PMTs exceeds an amplitude of 10 (before June 1997) or 8 (after June 1997) photoelectrons; in order to trigger the IACT system and to initiate the readout of data, at least two telescopes have to trigger simultaneously. Typical trigger rates are in the 10–16 Hz range. The PMT signals are digitized and recorded by 120 MHz Flash-ADCs. The telescope hardware is described by Hermann (1995); the trigger system and its performance are reviewed by Bulian et al. (1998); the calibration of the detector sensitivity is described in (Fraß et al. 1997), and the determination of the correct telescope pointing with 35 arc sec accuracy is described in (Pühlhofer et al. 1997).

3. Data sample and analysis tools

The analysis described in the following is based on 165 hours of data acquired between January 1st, 1997 and May 27th, 1998 with Mkn 421 altitudes larger than $45°$ above the horizon. Only data taken with all four IACTs during excellent weather conditions, i.e. clear sky and humidity below 90%, were used. Furthermore, data runs with a mean Cosmic Ray rate deviating by more than 21% from the expected value or with a mean width parameter per telescope deviating by more than 6% from the expected value were excluded from the analysis.

The Monte Carlo simulations used for the data analysis are described in detail in (Hemberger 1998; Konopelko et al. 1999). Changes of the trigger conditions, the mirror alignment and reflectivities, as well as in the PM sensitivities divide the data sample into eight phases of approximately uniform detector performance. For each of these eight phases, the detector simulations were adjusted to describe as closely as possible the hardware performance. Hereby information about the mirror alignment from point runs, the mirror reflectivities, the PMT sensitivities from the measured Cosmic Ray rates, and the measured single pixel trigger characteristics were taken into account (see Paper 1, 2 and references therein). The Monte Carlo fine tuning and the data quality were intensively tested using data from Mkn 501, Mkn 421, and from the Crab nebula, effectively validating all response functions relevant for the determination of γ-ray fluxes and γ-ray energy spectra (see Paper 1, 2, and Hofmann 1997). The current status of the Crab analysis with the HEGRA telescope system is described in (Konopelko et al. 1998).

The standard analysis methods described in detail in Paper 1 and 2 were used. Thus, spectral studies were performed with loose selection cuts, i.e. with a cut on the angular distance Θ of the reconstructed direction from the Mkn 421 direction $\Theta^2 < (0.22°)^2$ and a cut on the parameter "mean scaled width" with a cut value of 1.2. Loose cuts do not give an optimal signal to noise ratio but guarantee small systematic errors on the energy dependent cut efficiencies. The analysis uses an extended OFF-region for minimizing the statistical errors of the background estimate. A ring segment (of $180°$ opening angle), from $0.3°$ to $0.7°$ distance from the camera center, at the opposite side of the ON-region, has been chosen. The energy reconstruction required two IACTs within 200 m from the shower axis, each with more than 40 photoelectrons per image and a "distance" parameter of smaller than $1.7°$. Additionally, a minimal stereo angle larger than $20°$ was required.

The systematic uncertainties can be divided into two parts: into an uncertainty in the absolute energy scale, and into additional uncertainties in spectral shape (see Paper 2). The uncertainty in the absolute energy scale is 15%, dominated by a 10% uncertainty in the detector sensitivity. Additional uncertainties arise mainly due to the incomplete knowledge of the atmospheric conditions during the observations. The uncertainty in spectral shape is considerable in the threshold energy region, i.e. at energies below 1 TeV. Here the error is dominated by incomplete knowledge of the trigger behavior of the IACTs and by uncertainties in the reconstruction of γ-ray energy spectra based on Monte Carlo simulations at discrete zenith angles. Integral fluxes above a certain energy threshold were obtained by integrating the differential energy spectra above the threshold energy, rather than by simply scaling detection rates. By this means integral fluxes were computed without assuming a certain source energy spectrum.

For the data up to zenith angles of $30°$ (comprising altogether 126 h of data) spectral results are presented for energies above 500 GeV; for the 39 h of data with zenith angles between $30°$ and $45°$, an energy threshold of 1 TeV has been chosen. If
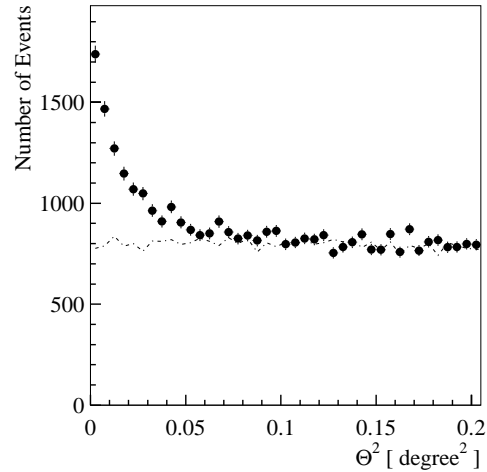
Fig. 1. The Mkn 421 excess from 1997–1998. The full circles show the events in the ON-region, the dashed line the events in the OFF-region (background region) after a loose "mean scaled width" cut and a software threshold of at least 40 photoelectrons in two or more telescopes.

not stated otherwise, the results presented in the following were derived from data with zenith angles below $30°$.

## 4. Experimental results

4.1. Time-averaged properties

The total excess from Mkn 421 is shown in Fig. 1. Using an angular cut of $\Theta^2 < (0.22°)^2$ the significance of the excess $((N_{\mathrm{on}} - N_{\mathrm{off}})/\sqrt{N_{\mathrm{on}} + N_{\mathrm{off}}})$ is 16σ before image cut and 26σ after the image cut. The total number of recorded γ-rays is about 8000 at hardware threshold. The time-averaged energy spectrum determined from the data with zenith angles smaller than $30°$ is shown in Fig. 2. The error bars show the statistical errors, and the hatched region shows the systematic uncertainty in spectral shape described above. Additionally, there is a 15% uncertainty in the absolute energy scale. From the lowest energies of 500 GeV to the highest energies detected at about 7 TeV, the spectrum can be described by a power law (Fig. 2, solid line)

$$\frac{d\mathrm{N}}{d\mathrm{E}} = (12.1 \pm 0.5_{\mathrm{stat}} \pm 4.3_{\mathrm{syst}}) \, 10^{-12} \times$$

$$(\mathrm{E}/\mathrm{TeV})^{(-3.09 \pm 0.07_{\mathrm{stat}} \pm 0.10_{\mathrm{syst}})} \, \mathrm{cm}^{-2}\mathrm{s}^{-1}\mathrm{TeV}^{-1} \,. \quad (1)$$

The 36% systematic error on the flux at 1 TeV takes into account the uncertainty in the shape of the spectrum and the 15% uncertainty in the energy scale. The χ^2-value of the fit, computed with the statistical errors only, is 23.5 for 10 degrees of freedom, corresponding to a chance probability for larger χ^2-values of 1%. Taking into account the systematic uncertainties in spectral shape, the result is surely compatible with a pure power law spectrum. Note, however, that a power law with an exponential cutoff:

$$d\mathrm{N}/d\mathrm{E} \propto (\mathrm{E}/\mathrm{TeV})^{(-2.5 \pm 0.4_{\mathrm{stat}})} \exp(-\mathrm{E}/\mathrm{E}_0) \quad (2)$$

with $\mathrm{E}_0 = 2.8 \left(^{+2.0}_{-0.9}\right)_{\mathrm{stat}}$ TeV, fits the data equally well (Fig. 2, dashed line). Here the χ^2-value, also computed with the statis-
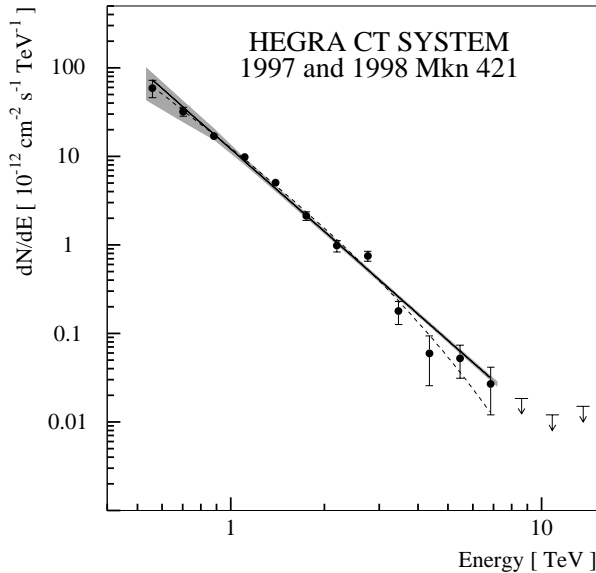
Fig. 2. The time-averaged 1997–1998 Mkn 421 energy spectrum. Vertical errors bars indicate statistical errors. The hatched area gives the estimated systematic uncertainty in spectral shape. Additionally, there is a 15% uncertainty in the absolute energy scale. The solid line shows a power law fit, the dashed line a power law with an exponential cut off (see text). Upper limits are at 2σ confidence level.
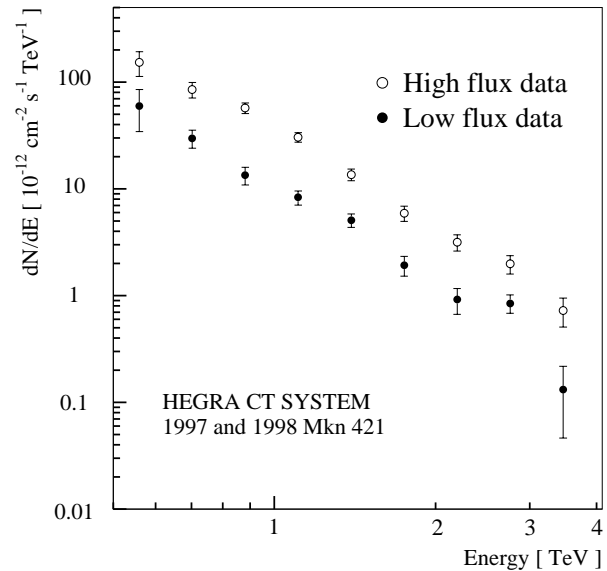
Fig. 3. The figure shows the energy spectrum for all days with a time-averaged differential flux at 1 TeV, between $5 \cdot 10^{-12}$ cm^{-2}s^{-1}TeV^{-1} and $15 \cdot 10^{-12}$ cm^{-2}s^{-1}TeV^{-1}, and above $30 \cdot 10^{-12}$ cm^{-2}s^{-1}TeV^{-1}, lower and upper curve respectively. The systematic errors are not shown here since they are expected to influence both spectra in the same way.

tical errors only, is 16.8 for 9 degrees of freedom with a chance probability for larger χ^2-values of 5%. The evaluation of the data from 30° to 45° zenith angles (39 h) gives similar results, although the statistics are very poor; the power law fit from 1 TeV to 5 TeV yields a differential spectral index of $-3.16 \pm 0.3_{\text{stat}}$.

The statistics do not permit inferences about temporal changes in the energy spectrum between 1997 and 1998: for 1997, a differential spectral index of $-3.28 \pm 0.20_{\text{stat}}$ is computed, and for 1998 it is $-3.00 \pm 0.05_{\text{stat}}$.

A possible correlation between absolute flux and spectral shape was searched for by determining the time-averaged energy spectrum for all days having a differential flux at 1 TeV between $5 \cdot 10^{-12}$ cm^{-2}s^{-1}TeV^{-1} and $15 \cdot 10^{-12}$ cm^{-2}s^{-1}TeV^{-1}, and above $30 \cdot 10^{-12}$ cm^{-2}s^{-1}TeV^{-1}. The two spectra are shown in Fig. 3 for all bins with reasonable statistical errors. A power law fit to the high state data gives a differential spectral index of $-2.98 \pm 0.09_{\text{stat}}$, while for the low state data we obtain $-3.02 \pm 0.12_{\text{stat}}$. There is thus no significant difference between the two spectra.

4.2. Diurnal results

Fig. 4 shows the 1997 and 1998 Mkn 421 light curve. Only statistical errors are shown. The systematic uncertainty in integral flux, dominated by the 15% uncertainty in the absolute energy scale, amounts to a 35% relative uncertainty. The relative systematic error is, to a good approximation, the same for all measurements. Mkn 421 was highly variable during 1997 and 1998;
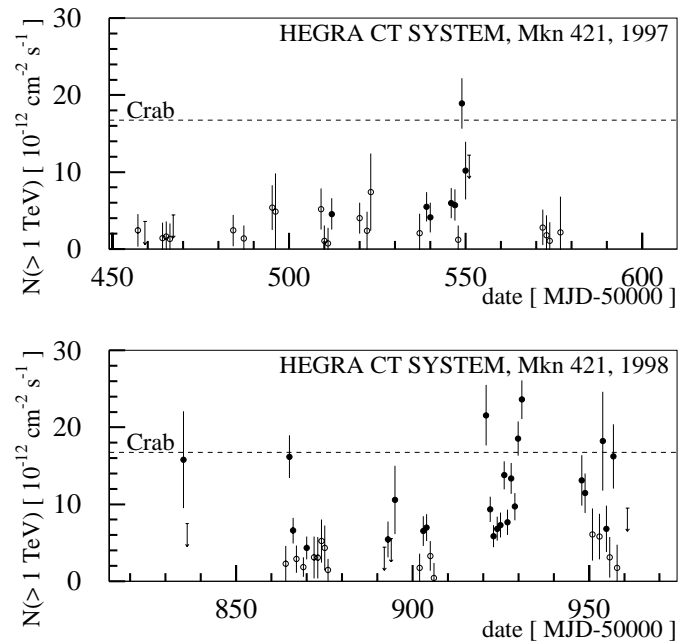
Fig. 4. The 1997 (upper panel) and 1998 (lower panel) Mkn 421 light curve, i.e., the integral fluxes above 1 TeV as a function of date. The upper light curve starts at MJD 50449 (1.1.1997) and ends at MJD 50610 (11.6.1997). The lower light curve starts at MJD 50814 (1.1.1998) and ends at MJD 50975 (11.6.1998). The full symbols show detections with at least 2σ significance and the open symbols are detections with less than 2σ significance. Only statistical errors are shown (systematic uncertainty in integral fluxes: 35% due to 15% uncertainty in the absolute energy scale). Upper limits are 2σ confidence level.
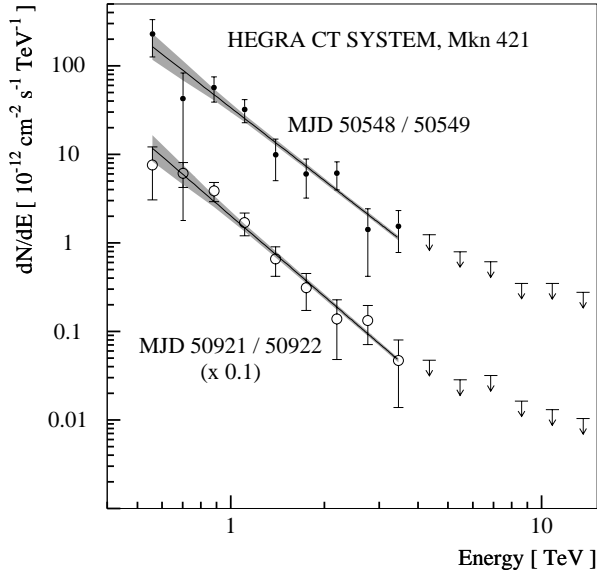
Fig. 5. Two diurnal Mkn 421 energy spectra. The lines show power law fits. The lower spectrum has been scaled by a factor of 0.1. The hatched area gives the estimated systematic uncertainty in spectral shape. The 15% uncertainty in the absolute energy scale is not shown here. Upper limits are at 2σ confidence level.

Table 1. HEGRA results for Mkn 421 on diurnal basis (1997 and 1998). Only the statistical errors are given. The systematic uncertainty in the flux at 1 TeV is about 35% and the systematic uncertainty in the spectral indices is about 0.10.

start[a]	Δt [b]	dN/dE (1 TeV)[c]	spectral index	$N(> 1$ TeV$)$[d]
50545.9181	2.67	13.48 +3.28 -3.06	−3.87 +0.47 -0.51	5.95 +- 1.96
50548.9648	1.61	33.51 +4.23 -4.34	−2.71 +0.21 -0.26	18.90 +- 3.28
50865.0528	1.61	26.42 +3.93 -3.87	−2.81 +0.27 -0.32	16.18 +- 2.78
50866.0482	2.57	9.07 +2.43 -2.46	−2.89 +0.48 -0.55	6.57 +- 1.67
50902.9772	2.06	4.91 +2.10 -2.03	−2.05 +0.48 -0.69	6.52 +- 1.93
50903.9649	2.59	9.62 +2.58 -2.75	−3.13 +0.41 -0.63	6.97 +- 1.76
50920.8784	0.97	32.85 +5.64 -5.36	−2.66 +0.28 -0.33	21.58 +- 3.94
50921.8776	3.44	20.02 +2.53 -2.24	−3.05 +0.21 -0.25	9.34 +- 1.63
50922.8790	3.01	8.55 +2.08 -2.20	−2.63 +0.33 -0.46	5.85 +- 1.41
50923.8785	2.94	12.70 +2.48 -2.69	−3.22 +0.43 -0.44	6.81 +- 1.55
50924.8804	3.21	9.43 +2.30 -2.28	−2.88 +0.36 -0.51	7.28 +- 1.61
50925.8812	3.12	22.11 +2.30 -2.48	−2.71 +0.15 -0.18	13.77 +- 1.82
50926.8814	3.05	16.75 +2.49 -2.74	−3.53 +0.31 -0.38	7.66 +- 1.64
50927.8839	2.93	30.35 +3.16 -2.86	−3.15 +0.20 -0.22	13.34 +- 2.01
50928.8824	2.92	16.75 +2.49 -2.74	−3.19 +0.31 -0.35	9.69 +- 1.76
50929.8848	2.81	34.18 +3.56 -2.60	−3.00 +0.15 -0.17	18.54 +- 2.24
50930.8845	2.72	37.00 +3.05 -3.49	−2.82 +0.13 -0.15	23.62 +- 2.51
50947.9065	0.97	18.14 +4.41 -4.39	−2.12 +0.44 -0.55	13.11 +- 3.28
50948.8937	1.44	13.48 +3.28 -3.46	−2.57 +0.31 -0.41	11.43 +- 2.58
50956.8999	0.83	29.75 +6.52 -7.20	−3.03 +0.53 -0.63	16.20 +- 4.17

[a] MJD
[b] duration of measurement in hours
[c] in (10^{-12}cm^{-2} s^{-1} TeV^{-1})
[d] in (10^{-12}cm^{-2} s^{-1})

the fluxes varied from an emission of a fraction of one Crab level to more than one Crab level. Most of the flares seemed to last one or two days. In 1998, from April 17th to April 28th (MJD 50920 – MJD 50931), a high state lasting for approximately ten days was observed. This flare coincided with a world-wide multiwavelength campaign lasting approximately from April 10 to April 30 (Takahashi et al. 1999; Urry 1999). A more detailed discussion of the HEGRA data from this campaign is given in the next subsection. During the whole 1997–1998 period no flares with fluxes in excess of two Crab levels were observed.

For days with long observation times or with strong source activity, diurnal differential spectra could be obtained. Two examples of spectra are shown in Fig. 5. The upper spectrum was acquired during 1.6 hours and the lower one during 3.4 hours. These diurnal spectra have statistics limited to energies below 4 TeV. In Table 1 the results of power law fits are summarized for all days with good statistics (3 sigma excess above 1 TeV). No highly significant evidence for spectral variability was found; the diurnal differential spectral indices are statistically consistent with the mean index of −3.1. The two most significant deviations from the mean index were found for April 22nd/23rd, 1998 (MJD 50925/50926) and April 27th/28th, 1998 (MJD 50930/50931), where the spectral indices of −2.71 and −2.82 deviated by 2.1σ and 1.8σ from the mean value, respectively.

4.3. The data of April 1998

As mentioned above, the data of April 1998 are of special interest since a world-wide multiwavelength campaign was performed with measurements in the radio, optical, and UV

regimes, at X-Ray energies (RXTE, BEPPO Sax, ASCA), at GeV energies, and at TeV energies.

In Fig. 6, the HEGRA integral fluxes above 500 GeV and above 1 TeV are shown (data up to 30° zenith angle in both plots). The flux varied by a factor of up to four. Note that all days of the multiwavelength campaign are included in Table 1, since the emission was high and the observation windows were large. In Fig. 7, the mean spectrum during the April campaign is shown. A power law fit yields a differential spectral index of $-3.03 \pm 0.08_{\text{stat}} \pm 0.10_{\text{syst}}$. The mean differential flux at 1 TeV was $(23.5 \pm 1.1_{\text{stat}} \pm 8.4_{\text{syst}})10^{-12}$ cm^{-2}s^{-1}TeV^{-1}, which roughly equals the Crab flux at 1 TeV. The χ^2-value computed with the statistical errors is 16.1 for 9 degrees of freedom, corresponding to a chance probability for larger χ^2-values of 6.5%.

4.4. Search for variability within individual nights

Temporal variability within individual nights was investigated using the integral fluxes above 500 GeV (data with zenith angles up to 30°) and above 1 TeV (data with zenith angles up to 45°). For the data of each night, the integral fluxes were determined with 15 min bins. For the first data selection the mean observation duration was 1.7 h per night; for the second one it is 25% higher, since data of larger zenith angles were included. Variability was searched for with a χ^2-analysis, fitting constant models to the integral flux rates and determining the chance probabilities for the resulting χ^2-values. For both threshold data samples the chance probabilities roughly distribute as expected in the absence of significant variability. For the 1 TeV threshold sample we find a marginally significant excess in three nights with chance probabilities smaller than 1%. Taking into
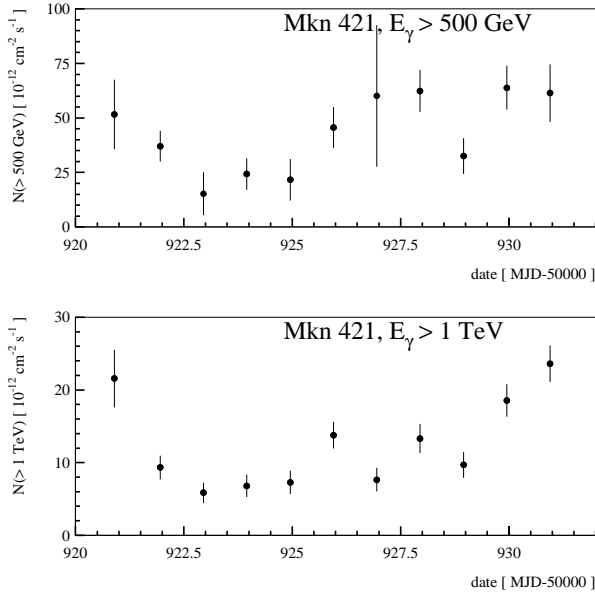
Fig. 6. Integral HEGRA fluxes for Mkn 421 during the world-wide multiwavelength campaign for a threshold energy of 500 GeV in the upper panel and a threshold energy of 1 TeV in the lower panel. Only statistical errors are shown. The statistical errors of the 500 GeV data sample are larger than for the 1 TeV data sample, since events near the detector threshold of 500 GeV, which were taken under larger zenith angles enter the integral flux with large weights. (systematic error on integral fluxes: 35% due to 15% uncertainty in the absolute energy scale)

account that 76 nights have been studied, the chance probability for finding such three nights is computed to be 4%. The integral fluxes above one TeV are shown in Fig. 8 for two nights. The lower panel shows one of the three nights with the most significant variability (May 21st/22nd, 1998, MJD 50954/50955). The examples exemplify that due to limited photon statistics, the search is only sensitive to strong flares. A preliminary analysis of Whipple data taken during the world-wide multiwavelength campaign indicated flux variability at energies above 2 TeV on a time scale of several hours (Maraschi et al. 1999a). No simultaneous data was taken with the IACT system of HEGRA.

5. Discussion

In this paper we present detailed temporal and spectral information about Mkn 421 during 1997 and 1998. The mean 1997–1998 differential flux at 1 TeV was about one half of the flux of the Crab nebula. The light curve shows several distinct flares with mean durations of typically one or two days and fluxes at 1 TeV of approximately the Crab level. During the world-wide multiwavelength campaign in 1998 we observed a 10 day phase of increased Mkn 421 activity with a differential flux at 1 TeV of one Crab level.

The time-averaged energy spectrum follows to a good approximation a power law with a differential spectral index (500 GeV to 7 TeV) of $-3.09\pm0.07_{\mathrm{stat}}\pm0.10_{\mathrm{syst}}$. Our result is consistent with earlier measurements of the differential spec-
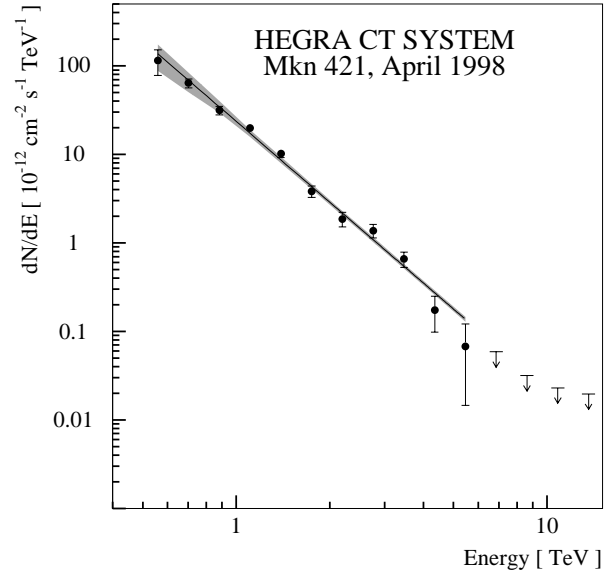

Fig. 7. The Mkn 421 spectrum during the April 1998 observation period (17.-28.04.1998). The solid line shows a power law fit. The hatched area gives the estimated systematic uncertainty in spectral shape. The 15% uncertainty in the absolute energy scale is not shown here. Upper limits are at 2σ confidence level.
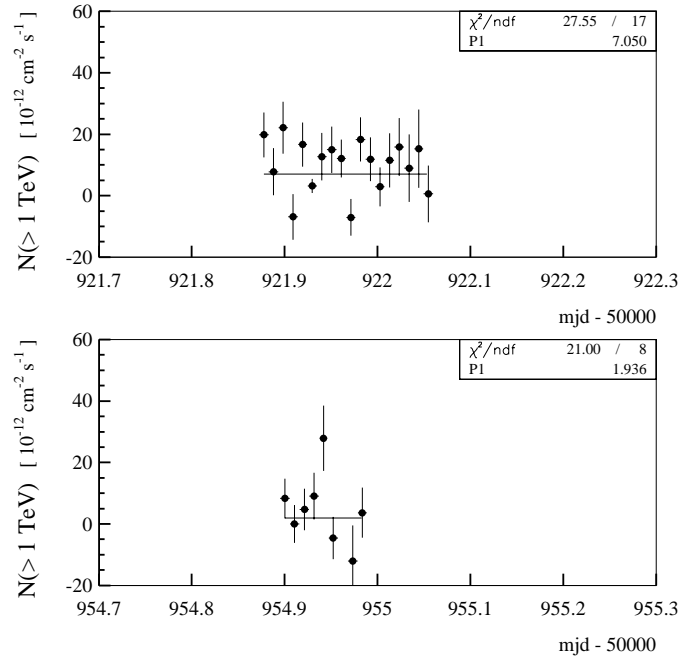
Fig. 8. The integral flux above 1 TeV as a function of time is shown for two nights. Each value has been determined with a 15 minute bin. Only statistical errors are shown (systematic error on integral fluxes: 35% due to 15% uncertainty in the absolute energy scale).

tral index during periods of moderate flux, i.e. $-3.6\pm1.0_{\mathrm{stat}}$ (at ≥1.2TeV) measured during the 1994/1995 observation period with the HEGRA CT1 telescope (Petry et al. 1996) and $-2.92\pm0.22_{\mathrm{stat}}\pm0.1_{\mathrm{syst}}$ measured during the 1995/1996 observation period with the Whipple telescope (Zweerink et al. 1997).
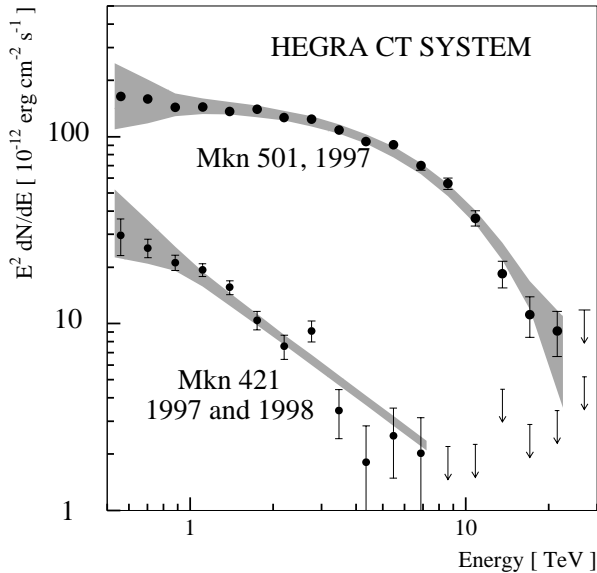
Fig. 9. The 1997 Mkn 501 and the 1997–1998 Mkn 421 spectral energy distributions. The hatched areas give the estimated systematic errors, except the 15% uncertainty in the absolute energy scale. Upper limits are at 2σ confidence level.

We did not find highly significant deviations from this mean spectrum, neither by dividing the data into a 1997 and a 1998 data sample, nor by dividing the data in a low and a high emission data set. Moreover, the diurnal spectra – some can be determined with an accuracy of 0.2 in the differential spectral index – are consistent with the mean spectrum.

The Whipple group reported an extraordinary Mkn 421 flare observed on May 7th, 1996 with an integral TeV flux of more than 5 Crab units and a flux increase by a factor of $\sim$2 within approximately 1 h (Gaidos et al. 1996), which allowed the determination of the differential spectral index during the flare with good statistical accuracy (Zweerink et al. 1997; Krennrich et al. 1999). An index of $-2.56 \pm 0.07_{\text{stat}} \pm 0.1_{\text{syst}}$ indicated a harder spectrum in the flaring state than in the quiescent state. Whereas our Mkn 421 spectra are consistent with a spectral index which is independent of time and absolute flux just as in the case of Mkn 501 (Paper 1), the Whipple spectrum during the extraordinary flare appears to be harder. Nevertheless, taking into account the statistical and systematic errors on the estimates of the photon power law index the effect of spectral hardening during the very strong flare is only marginally significant.

In our data we did not find strong evidence for flux-variability within individual nights, although the sensitivity for this search was limited due to short observation windows of approximately 2 h and the low levels of emission.

Due to the similar redshifts of Mkn 421 and Mkn 501 the comparison of their spectra promises insights into the intergalactic absorption by the DEBRA. In Fig. 9, the 1997–1998 Mkn 421 spectrum is compared to the 1997 Mkn 501 spectrum. During 1997 Mkn 501 was on average more than 7 times brighter than Mkn 421 at 1 TeV during 1997–1998. The Mkn 421 spectrum is much softer than the Mkn 501 spectrum. Between energies of

one and several TeV the differential spectral index is -3.1 for Mkn 421 and -2.2 for Mkn 501. Certainly, as discussed further below, due to the similar redshifts of both objects the difference has to be attributed to different intrinsic spectra and not to differences in the extinction by the DEBRA. In the Mkn 501 spectrum we recorded an exponential cutoff at 6.2 TeV, which could well be the result of intergalactic absorption by the DEBRA (see Paper 2 for a detailed discussion of possible origins of the exponential cutoff). As can be recognized from the fits to the Mkn 421 data of Eqs. 1 and 2, we cannot exclude an exponential cutoff for cutoff energies above $\simeq$2.8 TeV; this question will further be studied in future observations. In this presentation the Mkn 421 spectrum shows some curvature around 1 TeV. However, taking into account the systematic uncertainties in spectral shape (see hatched regions in Fig. 9) the curvature is not significant.

Since the DEBRA modifies the Mkn 421 and Mkn 501 TeV spectra in approximately the same way, the comparison of their spectra yields information about the intrinsic emission properties. Despite some similarities of both sources – the strong flux variability, the lack of strong spectral changes in the TeV emission, and the correlation of the emission strength in the X-ray and TeV energy bands (see e.g. Buckley et al. 1996; Takahashi et al. 1996; Aharonian et al. 1999c) – these two sources show significantly different energy spectra in both, the X-ray and TeV domains. Typically, the peak of the SED in the X-ray regime is found at lower energies for Mkn 421 than for Mkn 501 (see e.g. Maraschi et al. 1999b). The TeV spectra shown in Fig. 9 indicate that also the peak of the SED in the TeV-regime appears at lower energies in Mkn 421 than in Mkn 501. Within synchrotron Compton models this could be interpreted as significantly different parameters characterizing the γ-ray production, namely e.g. the Doppler factor of the emission volume, its size or the magnetic field, or the maximum energy of accelerated electrons. In addition, the steeper spectrum of Mkn 421 could be explained by internal absorption of the γ-rays due to pair production processes. Due to the large number of free parameters in even the simplest models, and the absence of comprehensive multiwavelength studies so far, it is difficult at this point to make firm conclusions about the contribution of each effect in the formation of the TeV spectra. The recent multiwavelength campaigns carried out for both sources, with simultaneous (to within a few hours) observations in different energy bands, hopefully will help to properly understand the physics of high energy processes in relativistic jets in these two sources.

References

Aharonian F.A., Akhperjanian A.G., Barrio J.A., et al., 1999a, A&A 342, 69 (Paper 1)

Aharonian F.A., Akhperjanian A.G., Barrio J.A., et al., 1999b, A&A 349, 11 (Paper 2)

Aharonian F.A., Akhperjanian A.G., Barrio J.A., et al., 1999c, A&A 349, 29

Bednarek W., Protheroe R.J., 1999, submitted to MNRAS

Blandford R.D., Levinson A., 1995, ApJ 441, 79

Bloom S.D., Marscher A.P., 1993, In: Friedlander M., Gehrels N., Macomb D.J. (eds.) AIP Conf. Proc. 280, Compton Gamma-Ray Observatory, AIP, New York, 578

Bradbury S.M., Deckers T., Petry D., et al., 1997, A&A 320, L5

Buckley J.H., Akerlof C.W., Biller S., et al., 1996, ApJ 472, L9

Bulian N., Daum A., Hermann G., et al., 1998, Astropart. Phys. 8, 223

Coppi P.S., 1997, In: Ostrowski M., Sikora M., Madejski G., Begelman M. (eds.) Cracow Workshop on Relativistic Jets in AGNs, Jagellonian University Press, p. 333

Coppi P.S., Aharonian F.A., 1999, ApJL, in press

Daum A., Hermann G., Heß M., et al., 1997, Astropart. Phys. 8, 1

Dermer C.D., Schlickeiser R., 1994, ApJS 90, 945

Fossati G., Maraschi L., Celotti A., Comastri A., Ghisellini G., 1998, MNRAS 299, 433

Fraß A., Köhler C., Hermann G., Heß M., Hofmann W., 1997, Astropart. Phys. 8, 91

Gaidos J.A., Akerlof C.W., Biller S.D., et al., 1996, Nat 383, 319

Ghisellini G., Maraschi L., Dondi L., 1996, A&AS 120, 503

Gould J., Schréder, 1966, Phys. Rev. Lett. 16, 252

Hartman R.C., Bertsch D.L., Bloom S.D., et al., 1999, ApJS, in press

Hemberger M., 1998, Ph.D. Thesis, Heidelberg

Hermann G., 1995. In: Cresti M. (ed.) Procs. Towards a Major Atmospheric Cherenkov Detector IV, Padova, p. 396

Hofmann W., 1997. In: De Jager O.C. (ed.) Procs. Towards a Major Atmospheric Cherenkov Detector V, Kruger Park, South Africa, p. 284

Konopelko A. (HEGRA collaboration), 1998, In: Proc. 14th Europ. Cosmic Ray Symp., Madrid, in press

Konopelko A., Hemberger M., Aharonian F., et al., 1999, Astropart. Phys. 10, 275

Krennrich F., Biller S.D., Bond I.H., et al., 1999, ApJ 511, 149

Mannheim K., 1993, A&A 269, 67

Maraschi L., Fossati G., Tavecchio F., et al., 1999a, In: Weekes T.C., Catanese M. (eds.) Proc. the Veritas Workshop on the TeV Astrophysics of Extragalactic Objects, Astroparticle Physics, in press

Maraschi L., Chiappetti L., Fossati G., Pian E., Tavecchio F., 1999b, In: Proc. 32nd COSPAR Meeting, Nagoya 1998, in press

Mastichiadis A., Kirk J.G., 1997, A&A 320, 19

Mirzoyan R., Kankanian R., Krennrich F., et al., 1994, NIM A 315, 513

Petry D., Bradbury S.M., Konopelko A., et al., 1996, A&A 311, L13

Protheroe R.J., Bhat C.L., Fleury P., et al., 1998, In: Proc. 25th ICRC Vol. 8, Durban, p. 317

Pühlhofer G., Daum A., Hermann G., et al., 1997, Astropart. Phys. 8, 101

Punch M., Akerlof C.W., Cawley M.F., et al., 1992, Nat 358, 477

Quinn J., Akerlof C.W., Biller S., et al., 1996, ApJ 456, L83

Rauterberg G., Müller N., Deckers T. (HEGRA collaboration), 1995, In: Proc. 24th ICRC, Rome, 3, 460

Sikora M., 1997, In: Dermer C., Strickman M., Kurfess J. (eds.) Proc. 4th Compton Symposium, AIP Conf. Proc., 494

Sikora M., Begelman M.C., Rees M.J., 1994, ApJ 421, 153

Stecker F.W., De Jager O.C., Salamon M.H., 1992, ApJ 390, L49

Takahashi T., Tashiro M., Madejski G., et al., 1996, ApJ 470, L89

Takahashi T., Madejski G., Kubo H., 1999, In: Weekes T.C., Catanese M. (eds.) Proc. the Veritas Workshop on the TeV Astrophysics of Extragalactic Objects. Astroparticle Physics, in press

Ulrich M.H., Maraschi L., Urry C.M., 1997, ARA&A 35, 445

Urry C.M., 1999, In: Weekes T.C., Catanese M. (eds.) Proc. the Veritas Workshop on the TeV Astrophysics of Extragalactic Objects. Astroparticle Physics, in press

Zweerink J.A., Akerlof C.W., Biller S.D., et al., 1997, ApJ 490, L141